

Stable and efficient evaluation of periodized Green’s functions for the Helmholtz equation at high frequencies

Harun Kurkcu^{a,*} and Fernando Reitich^a

^a*School of Mathematics, University of Minnesota, Minneapolis, MN 55455, United States*

Abstract

A difficulty that arises in the context of infinite d -periodic rough-surface scattering relates to the effective numerical evaluation of the corresponding “quasi-periodic Green function” G_{qp} . Due to its relevance in a variety of applications, this problem has generated significant interest over the last 40 years, and a variety of numerical methods have been devised for this purpose. None of these methods to evaluate G_{qp} however, were designed for high-frequency calculations. As a result, in this regime, these methods become prohibitively expensive and/or unstable. Here we present a novel scheme that can be shown to outperform every alternative numerical evaluation procedure and is especially effective for high-frequency calculations. Our new algorithm is based on the use of some exact integrals that arise on judicious manipulation of the integral representation of G_{qp} and which reduce the overall problem to that of evaluation of a sequence of simpler integrals that can be effectively handled by standard quadrature formulas. We include a variety of numerical results that confirm that, indeed, our algorithm compares favorably with alternative methods.

Key words: Green’s function periodic domain, rough-surface, high-frequency, free-space, Helmholtz equation.

1 Introduction

The analysis of (acoustic/electromagnetic/elastic) wave scattering off extended rough-surfaces arises naturally in a variety of engineering and industrial ap-

* Corresponding author.

Email addresses: kurkcu@math.umn.edu (Harun Kurkcu),
reitich@math.umn.edu (Fernando Reitich).

plications including, for instance, remote sensing [1], underwater acoustics [2], wireless communications [3], radar imaging [4], and micro-optics [5]. As a result, significant effort has been devoted in the last few decades to develop models and computer algorithms whose numerical implementation can lead to faithful and efficient simulations of rough-surface scattering [6]. These schemes can be based on asymptotic treatments [7] or on rigorous approximations that rely on finite-elements [8], finite-differences [9], or integral equations [10]. Among these methods, those based on integral-equation formulations offer significant advantages, such as that of dimensional reduction in surface scattering applications, of automatic enforcement of radiation conditions and of the potential for accelerated evaluations [11,12]. This paper is devoted to the introduction of a new scheme for the evaluation of the appropriate Green functions that allow for rough-surface scattering calculations within integral-equation formulations.

More precisely, these non-standard Green functions emerge as a result of the specifics of the geometries that arise in the aforementioned applications. Specifically, in many such scenarios the range of the scatterer’s surface (a section of terrain, an ocean surface, a diffraction grating, etc.) is such that effects due to its termination are negligible, and an accurate representation can be garnered from the assumption that the surface is of infinite extent. Typically then the additional hypothesis of (possibly large) periodicity is posited which tends to simplify the mathematical treatment by allowing for evaluations to be performed in a single base period. For scattering calculations, however, a problem still remains even under this hypothesis as interactions between remote portions of the surface and this base period need to be accounted for. In the context of integral-equation formulations of the scattering problem, these interactions can be resolved by consideration of a (quasi-) periodized Green function G_{qp} [13] constructed as a sum of (periodic) translates of the free-space fundamental solution. The long-range character of the latter then results in a slow decay of the series defining G_{qp} and thus makes it challenging to evaluate. In what follows we present a novel approach to the stable evaluation of G_{qp} that allows for the efficient attainment of exceptional accuracies at very high-frequencies.

The evaluation of the periodized Green function constitutes, in fact, the main impediment in the design of accurate and effective integral-equation solvers for infinite rough-surface scattering. As such, this problem has attracted significant attention over the last 40 years and it has resulted in a variety of numerical procedures [14]. Most notable among these are those based on spectral [15–18] and integral [19–21] representations, on Kummer [22–24] and Ewald transforms [19,25] and on lattice sums [24,26,27]; see §2 for a discussion on each of these. Although these methods may provide a means to accurately evaluate $G_{qp}(x, y)$ at low frequencies, they become uniformly prohibitively expensive and/or unstable at higher frequencies, e.g. where the height y of the

evaluation point relative to the pole exceeds a multiple of $\sqrt{\lambda d}$ where d is the period and λ the wavelength of oscillation; see §3.

The method we introduce herein, on the other hand, can effectively provide solutions at very high-frequencies, while remaining competitive with the optimal choices of currently available schemes throughout their domain of applicability. Briefly, the method begins with an integral formula [19] for $G_{\text{qp}}(x, y)$ which represents it as an integral of an exponentially decaying function $f(x, y; u)$ for $u \geq 0$. At low frequencies (specifically, for $y = \mathcal{O}(\sqrt{\lambda d})$ as $\lambda \rightarrow 0$) the function f and its derivatives remain bounded and a standard quadrature can provide an efficient means to evaluate the integral. As the frequency increases, on the other hand, the integrand f displays progressively larger and more rapid oscillations which cancel out to produce a significantly smaller integrated value. In this case then, classical quadratures tend to be unstable and unable to accurately determine the values of G_{qp} . To overcome these difficulties our scheme is based on polynomial expansion of quotients of f and suitably chosen functions to allow for explicit evaluations, and on judicious integration by parts in order to improve stability and reduce the computational cost. This procedure results in a representation of the Green function in terms of an explicitly computable series and a remainder integral that can be computed in times that are independent of the frequency. Moreover, we also show that subtle rearrangements of the series can be effected to simplify its expression and which result in further and significant improvements in the accuracy and efficiency of the overall scheme.

The rest of the paper is organized as follows. First, and for the sake of completeness, in §2 we briefly review the most popular methods that have been devised to compute G_{qp} , including those based on spectral and integral representations, on Kummer and Ewald transforms and on lattice sums. Then, in §3, we discuss the problems that arise with each of these as the frequency increases, and we explain the origins of the corresponding increase in computational cost and/or the deterioration of their stability properties. Section §4 is devoted to the presentation of our new algorithm, including the derivation of a new series representation and the manipulations that lead to favorable rearrangements. Finally in §5 we present a variety of numerical results that confirm that our new procedure allows for calculations of a quality and efficiency comparable to that attainable by state-of-the-art methodologies where these are applicable while also enabling evaluations for frequencies that lie well-beyond those that can be treated with these techniques.

2 A review of existing algorithms

In this section, and for the sake of completeness, we briefly review the most popular and effective numerical methods that have been devised to compute G_{qp} . To begin, we recall the definition of G_{qp} , which depends on the (incidence of the) basic scattering problem under consideration. More precisely if, for instance, the (infinite) surface $y = g(x)$ acts as a sound-soft barrier for a (plane wave) incidence, the scattered field $u(x, y)$ will satisfy

$$\begin{cases} \Delta u(x, y) + k^2 u(x, y) = 0 & \text{for } y > g(x) \\ u(x, y)|_{y=g(x)} = -e^{i\alpha x - i\beta y}|_{y=g(x)} \\ u(x, y) \text{ satisfies the "upward propagating condition"} \end{cases} \quad [28].$$

As can be easily verified [13], if the surface $y = g(x)$ is d -periodic, the scattered field will necessarily be " α quasi-periodic", that is

$$u(x + d, y) = e^{i\alpha d} u(x, y)$$

or, equivalently,

$$u(x, y)e^{-i\alpha x} \text{ is } d\text{-periodic.}$$

The relevant fundamental solution $G_{\text{qp}}(x, y)$ then will satisfy

$$\begin{cases} \Delta G_{\text{qp}}(x, y) + k^2 G_{\text{qp}}(x, y) = \delta(y) \sum_{n=-\infty}^{\infty} e^{i\alpha nd} \delta(x - nd) \\ G_{\text{qp}}(x, y) \text{ satisfies the upward propagating condition} \end{cases} \quad (1)$$

and a variety of representations for it are thus possible, each giving rise to opportunities for numerical approximation. These representations include:

1. Spatial representation: this follows from the explicit knowledge of the free-space Green function $G(x, y)$, i.e. the solution to (1) in the absence of periodicity, that is with a single point source at the origin ($n = 0$ in the notation of (1)). In this case, it is well-known [13] that the solution is given by

$$G(x, y) = -\frac{i}{4} H_0^{(1)}(kr)$$

where $H_0^{(1)}$ is the zeroth order Hankel function of the first kind and $r = \sqrt{x^2 + y^2}$. The (quasi) periodic placement of point sources that defines G_{qp} then readily implies that this can be represented as a sum of translates of $G(x, y)$, that is

$$G_{\text{qp}}(x, y) = -\frac{i}{4} \sum_{n=-\infty}^{\infty} e^{i\alpha nd} H_0^{(1)}(k\sqrt{(x - nd)^2 + y^2}) \quad (2)$$

which we shall refer to as the “spatial representation”. Note that the slow decay of the Hankel function translates into a slow decay of the series in (2) which, in fact, does not converge absolutely.

2. Spectral representation: this corresponds to the Fourier series representation of the (quasi) periodic function G_{qp} [15], which can be easily derived using Poisson’s summation formula. Specifically, this “spectral representation” takes the form

$$G_{\text{qp}}(x, y) = \frac{1}{2id} \sum_{n=-\infty}^{\infty} \frac{e^{i(\alpha_n x + \beta_n |y|)}}{\beta_n} \quad (3)$$

where

$$\alpha_n = \alpha + \frac{2\pi n}{d} \text{ and } \beta_n = \sqrt{k^2 - \alpha_n^2}.$$

In contrast with the representation in (2) the series in (3) converges exponentially. However the exponential decay only manifests itself beyond $\pm n = \pm(k \mp \alpha)/p$, and it deteriorates with decreasing $|y|$.

3. Kummer transformation: As we said, the terms in the spatial representation decay slowly, and so does the spectral series if $|y|$ is small. The Kummer transformation [22–24] seeks to accelerate their convergence by (adding and subtracting their asymptotic behavior and using closed form expressions for the series that arise from the latter. In the case of the spectral representation, for instance, we have that for large n

$$\beta_n = i|n|p \left(1 + \frac{\alpha \text{sgn}(n)}{|n|p} - \frac{k^2}{2n^2 p^2}\right) + \mathcal{O}(|n|^{-2}), \quad (4)$$

$$\frac{1}{i\beta_n} = -\frac{1}{|n|p} \left(1 - \frac{\alpha}{np} + \frac{k^2 + 2\alpha^2}{2n^2 p^2}\right) + \mathcal{O}(|n|^{-4}), \quad (5)$$

and therefore

$$\frac{e^{i\beta_n |y|}}{i\beta_n} \sim c_n \equiv -\frac{e^{-(|n|p + \alpha \text{sgn}(n))|y|}}{|n|p} \left(1 - \frac{\alpha}{np} + \frac{k^2 |y|}{2|n|p}\right)$$

where

$$p = \frac{2\pi}{d}.$$

From this, it follows that we can write

$$G_{\text{qp}}(x, y) = \frac{1}{2id} \left[\frac{e^{i\alpha_0 x} e^{i\beta_0 |y|}}{\beta_0} + \sum_{n \in \mathbb{Z}^*} e^{i\alpha_n x} \left(\frac{e^{i\beta_n |y|}}{\beta_n} + \frac{e^{-(|n|p + \alpha \text{sgn}(n))|y|}}{|n|p} \times \left\{ 1 - \frac{\alpha}{np} + \frac{k^2 |y|}{2|n|p} \right\} \right) + S_a \right] \quad (6)$$

where $\mathbb{Z}^* = \mathbb{Z} \setminus \{0\}$ and, due to the differencing, now the terms in the series decay as $\frac{e^{-|ny|p}}{n^3}$ rather than as $\frac{e^{-|ny|p}}{n}$ as in the original representation. The

sum of the series defining S_a , on the other hand, can be found in terms of standard functions; explicitly, letting $z = |y| + ix$, we have

$$\begin{aligned}
S_a &= \sum_{n \in \mathbb{Z}^*} c_n e^{i\alpha n x} \\
&= e^{-\alpha|y|} \sum_{n=1}^{\infty} \frac{e^{-npz}}{np} \left(1 - \frac{\alpha}{np} + \frac{k^2|y|}{2np}\right) + e^{\alpha|y|} \sum_{n=1}^{\infty} \frac{e^{-np\bar{z}}}{np} \left(1 + \frac{\alpha}{np} + \frac{k^2|y|}{2np}\right) \\
&= e^{-\alpha|y|} \left[\frac{1}{p} Li_1(e^{-p\bar{z}}) - \left(\frac{\alpha}{p^2} - \frac{k^2|y|}{2p^2}\right) Li_2(e^{-p\bar{z}}) \right] \\
&\quad + e^{\alpha|y|} \left[\frac{1}{p} Li_1(e^{-pz}) + \left(\frac{\alpha}{p^2} + \frac{k^2|y|}{2p^2}\right) Li_2(e^{-pz}) \right]
\end{aligned}$$

where \bar{z} denotes the complex conjugate of z and the polylogarithm function $Li_s(z)$ is defined by

$$Li_s(z) = \sum_{n=1}^{\infty} \frac{z^n}{n^s}.$$

Clearly, this acceleration process can be repeated by adding terms to the expansions (4) and (5) in order to make the series converge with an arbitrary order provided, of course, that $|n| > (k - \alpha)/p$.

4. Lattice sums method: this method [24,26,27] relies on the use of the addition theorem [29] to accelerate the convergence of the series (2) in the spatial representation. In detail, if (r, θ) denote the polar coordinates of the point (x, y) , then for $0 \leq r < d$ we can write

$$\begin{aligned}
G_{\text{qp}}(x, y) &= -\frac{i}{4} \left[H_0^{(1)}(kr) + \sum_{n \in \mathbb{Z}^*} e^{in\alpha d} H_0^{(1)}(k|(x, y) - (nd, 0)|) \right] \\
&= -\frac{i}{4} \left[H_0^{(1)}(kr) + \sum_{n \in \mathbb{Z}^*} e^{in\alpha d} \sum_{l=-\infty}^{\infty} H_l^{(1)}(k|n|d) e^{-il\varphi_n} J_l(kr) e^{-il\theta} \right]
\end{aligned}$$

where φ_n is the polar angle of the point $(nd, 0)$, that is

$$\varphi_n = \begin{cases} \pi & \text{if } n > 0, \\ 0 & \text{if } n < 0. \end{cases}$$

Exchanging the order of summation then we have

$$G_{\text{qp}}(x, y) = -\frac{i}{4} \left[H_0^{(1)}(kr) + \sum_{l=-\infty}^{\infty} S_l(k, d) J_l(kr) e^{-il\theta} \right] \quad (7)$$

where the ‘‘lattice sums’’ S_l are given by

$$\begin{aligned}
S_l(k, d) &= \sum_{n \in \mathbb{Z}^*} e^{in\alpha d} H_l^{(1)}(k|n|d) e^{-il\varphi_n} \\
&= \sum_{n \in \mathbb{Z}^*} e^{in\alpha d} J_l(k|n|d) e^{-il\varphi_n} + i \sum_{n \in \mathbb{Z}^*} e^{in\alpha d} Y_l(k|n|d) e^{-il\varphi_n} \quad (8) \\
&\equiv S_l^j(k, d) + iS_l^y(k, d).
\end{aligned}$$

Note that the convergence of the sum in (7) is exponential in the index l , and the problem in fact reduces to the design of suitable schemes for the evaluation of the sums in (8); see [24,26,27] and § 3.

5. Ewald transformation: [19,25] is based on the integral representation

$$-\frac{i}{4} H_0^{(1)}(kr) = \frac{1}{2\pi} \int_0^\infty \frac{e^{-r^2 s^2 + k/(4s^2)}}{s} ds \quad (9)$$

to accelerate the convergence of the spatial representation series in (2). Here, s is a complex variable, and the complex contour of integration is to be taken $\pi/4 \leq \arg(s) \leq 3\pi/4$ for $s \rightarrow 0$ and $-\pi/4 < \arg(s) < \pi/4$ for $s \rightarrow \infty$; see [30] and Figure 1. In terms of the integral in (9), this series can be written as

$$G_{\text{qp}}(x, y) = \frac{1}{2\pi} \sum_{n=0}^\infty e^{i\alpha nd} \int_0^\infty \frac{e^{-r_n^2 s^2 + k/(4s^2)}}{s} ds$$

where $r_n = \sqrt{(x - nd)^2 + y^2}$. Alternatively, for any fixed value of E , we have

$$G_{\text{qp}}(x, y) = G_1 + G_2$$

where

$$G_1 = \frac{1}{2\pi} \sum_{n=0}^\infty e^{i\alpha nd} \int_0^E \frac{e^{-r_n^2 s^2 + k/(4s^2)}}{s} ds \quad \text{and} \quad G_2 = \frac{1}{2\pi} \sum_{n=0}^\infty e^{i\alpha nd} \int_E^\infty \frac{e^{-r_n^2 s^2 + k/(4s^2)}}{s} ds. \quad (10)$$

Next, Poisson’s summation formula applied to G_1 gives

$$G_1 = \frac{1}{2id} \sum_{n=-\infty}^\infty \frac{1}{\beta_n} e^{i\alpha_n x} \left[e^{i\beta_n |y|} \operatorname{erfc}\left(\frac{i\beta_n d}{2E} + \frac{Ey}{d}\right) + e^{-i\beta_n |y|} \operatorname{erfc}\left(\frac{i\beta_n d}{2E} - \frac{Ey}{d}\right) \right] \quad (11)$$

where the complementary error function is defined by

$$\operatorname{erfc}(z) = 1 - \operatorname{erf}(z) = \frac{2}{\sqrt{\pi}} \int_z^\infty e^{-u^2} du,$$

and the terms in the series decay exponentially.

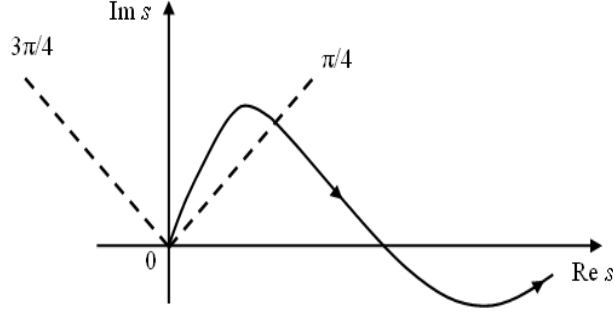


Fig. 1. Path of integration in (9): $\pi/4 \leq \arg(s) \leq 3\pi/4$ for $s \rightarrow 0$ and $-\pi/4 < \arg(s) < \pi/4$ for $s \rightarrow \infty$.

To deal with G_2 , we begin with a change of variables $u = s^2$ leading to

$$G_2 = \frac{1}{2\pi} \sum_{n=0}^{\infty} e^{i\alpha nd} \left(\frac{1}{2} \int_{E^2}^{\infty} \frac{e^{-r_n^2 u} e^{k/(4u)}}{u} du \right).$$

Then, using

$$e^{k^2/(4u)} = \sum_{n=0}^{\infty} \frac{(k/2)^{2n}}{u^n n!}$$

and letting $t = u/E^2$, it follows that

$$G_2 = -\frac{1}{4\pi} \sum_{n=-\infty}^{\infty} e^{i\alpha nd} \sum_{m=0}^{\infty} \frac{1}{n!} \left(\frac{kd}{2E} \right)^{2m} E_{m+1} \left(\frac{E^2 r_n^2}{d^2} \right) \quad (12)$$

where the n th order exponential integral $E_n(x)$ is defined by

$$E_n(x) = \int_1^{\infty} u^{-n} e^{-xu} du$$

so that, once again, the terms in the series (12) decay exponentially with increasing index m .

The combined exponential decay of the series (11) and (12) make this into a very efficient method for moderate values of k . In this case, it can be shown that the optimal choice of E is $E = \frac{\pi}{d}$, in which case both series converge at the same asymptotic rate [25]. As we show in §3, however, this choice of the parameter E leads to unstable evaluations and must be modified to ensure the boundedness of the terms in the series and this, in turn, leads to a computational cost that is similar to that of evaluation of standard spectral series (3).

6. Integral representation: There are several integral representations of the fundamental solution [19–21] wherein G_{qp} is represented as improper integrals of functions with a varying degree of singularity, ranging from square-root to Cauchy principal value. Among the former, for instance, such a

representation can be derived from the spatial form (2) using geometric series expansions and the inverse Laplace transform. More precisely, using

$$\sum_{n=0}^{\infty} e^{-ian} e^{nu} = \frac{e^{-ia}}{e^u - e^{-ia}},$$

multiplying both sides by a function f and integrating from 0 to ∞ we obtain

$$\sum_{n=0}^{\infty} e^{-ian} e^{nu} F(n) = e^{-ia} \int_0^{\infty} \frac{f(u)}{e^u - e^{-ia}} du$$

where $F(n)$ is the Laplace transform of $f(u)$. From this, and using the inverse Laplace transform formula

$$L^{-1}\{e^{in} H_0^{(1)}([n^2 + a^2]^{1/2})\} = i \frac{\cos(a\sqrt{u^2 - 2iu})}{\sqrt{u^2 - 2iu}}$$

it readily follows from (2) that

$$G_{\text{qp}}(x, y) = -\frac{i}{4} H_0^{(1)}(kr) - \frac{1}{\pi} I \quad (13)$$

where

$$I = \int_0^{\infty} \left[\frac{e^{kx(u^2-i)}}{e^{-i\alpha d + kd(u^2-i)} - 1} + \frac{e^{-kx(u^2-i)}}{e^{i\alpha d + kd(u^2-i)} - 1} \right] \frac{\cos(iky u \sqrt{u^2 - 2i})}{\sqrt{u^2 - 2i}} du. \quad (14)$$

At low frequencies (specifically, for $y = \mathcal{O}(\sqrt{\lambda d})$ as $\lambda \rightarrow 0$) the integrand and its derivatives remain bounded and a standard quadrature can provide an efficient means to evaluate the integral. Indeed near the singularity, that is for (x, y) near the origin, and for moderate frequencies this representation can be shown to be a most effective method. As the frequency increases, on the other hand, the integrand displays progressively larger and more rapid oscillations which cancel out to produce a significantly smaller integrated value.

3 High-frequency problems

In this section, we discuss the difficulties that arise in connection with attempts to use each of the methods described in §2 to evaluate the Green function for increasingly large frequencies. As we explain, these difficulties are associated, in each case, with an increase in computational cost and/or the deterioration of their stability properties whose origins we briefly discuss.

1. Spatial representation: the difficulties related to this method are independent of the frequency and are uniformly severe. As we mentioned, these

problems are due to the slow decay of the terms in the series (2) that follows from the asymptotic formula

$$H_0^{(1)}(z) \sim \sqrt{\frac{2}{\pi z}} e^{i(z - \frac{\pi}{4})} \quad \text{for } 1 \ll z \text{ [29, Equation 9.2.3].}$$

which implies that

$$G_{\text{qp}} = \sum_{n=-\infty}^{\infty} e^{i\alpha nd} H_0^{(1)}(k\sqrt{(x-nd)^2 + y^2}) \sim \sum_{n \in \mathbb{Z}^*} e^{i(knd + \alpha nd - \frac{\pi}{4})} \sqrt{\frac{2}{\pi knd}} + e^{i(kr - \frac{\pi}{4})} \sqrt{\frac{2}{\pi kr}}$$

independently of the wavelength of oscillation. Although this behavior suffices to deem the approach uncompetitive, a further problem arises at high-frequencies in connection with the accurate evaluation of the Hankel functions for large arguments.

2. Spectral representation: although this method can be shown to be the most stable among the ones we review here, its cost can become prohibitive at large frequencies. As we mentioned above, this is due to the fact that the onset of exponential decay of the terms in the series (3) occurs at $\pm n = \pm(k \mp \alpha)/p$. More precisely, for $N = \pm(k \mp \alpha)/p \pm m$, where $m > 0$, we have

$$i\beta_N |y| = i\sqrt{k^2 - (k + mp)^2} |y| = -\sqrt{2kmp + (mp)^2} |y|$$

which implies a computational cost of at least

$$2\frac{k - \alpha}{p} + \frac{2}{p|y|(\sqrt{ky^2 + 1} + k|y|)}$$

which may be large if either k is large or $|y|$ is small.

3. Kummer transform: while, as we have explained, the Kummer transformation generically mollifies the problems associated with the computational cost of the spectral representation, its stability properties at high-frequencies deteriorate significantly. This is largely due to the fact that, for large wavenumbers (precisely for $1 \ll \frac{k^2 y}{2p}$), the terms in the first series in the right hand side of (6) become large for small values of the index n . As a result the overall value of this series, and therefore also that of S_a in (6), becomes substantially larger than the value of the Green function; more precisely, we have

$$1 \ll S_a \sim \frac{k^2 |y|}{2p} \quad \text{and} \quad G_{\text{qp}} \sim \frac{1}{\sqrt{kd}} \ll 1. \quad (15)$$

This disparity thus leads to a loss of accuracy on evaluation of the right hand side of (6).

4. Lattice Sums Method: There are two different problems associated with the lattice sums method at high-frequencies relating, respectively, to the computational cost of evaluation of the series (7) and to the cost and stability of the calculation of the lattice sums $S_l(k, d)$. More precisely, in connection with the first problem and to elucidate the convergence properties of the series in (7) we appeal to the Debye asymptotic formula [29, Eq. (9.3.23)]

$$J_\nu(v + zv^{1/3}) \sim \frac{2^{1/3}}{v^{1/3}} \text{Ai}(-2^{1/3}z) \text{ for } z = \mathcal{O}(1) \text{ as } |v| \rightarrow \infty$$

where the Airy function behaves like

$$\text{Ai}(x) \sim \frac{e^{-2/3x^{3/2}}}{2\sqrt{\pi}x^{1/4}} \text{ for } x \text{ large.}$$

Letting

$$z = -\frac{n}{(kr+n)^{1/3}}$$

then, this implies that

$$J_{kr+n}(kr) \sim \frac{2^{1/3}}{(kr+n)^{1/3}} \text{Ai}\left(\frac{2^{1/3}n}{(kr+n)^{1/3}}\right) \sim \frac{e^{-2\sqrt{2}/3 \frac{n^{3/2}}{(kr+n)^{1/2}}}}{2^{3/4}\sqrt{\pi}(krn+n^2)^{1/4}}.$$

Since, on the other hand, the coefficients $S_l(k, d)$ oscillate as a function of l for any fixed wavenumber and period (see Figure 2), we conclude that the series in (7) must be truncated at a number N that cannot be smaller than

$$kr + (kr \log(2\epsilon))^{\frac{1}{3}} \quad (16)$$

for the given precision ϵ .

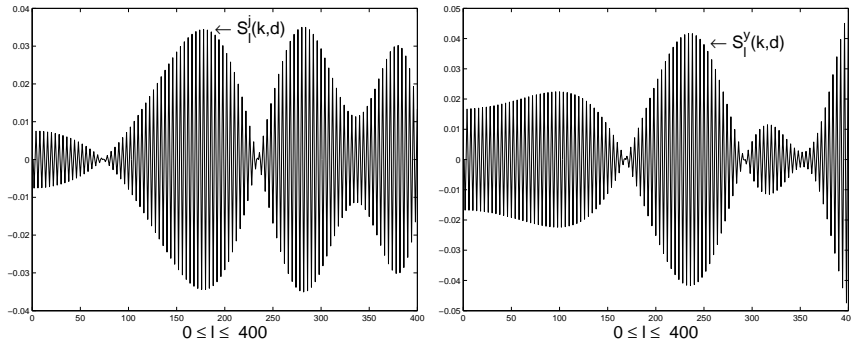


Fig. 2. Plots of the real and imaginary parts of the lattice sums $S_l(k, d) = S_l^j(k, d) + iS_l^y(k, d)$ in (7), (8) as functions of the order l . Left: $S_l^j(k, d)$, Right: $S_l^y(k, d)$; $k = 10^3 + 0.2$, $d = 2\pi$ and $\alpha = 0$.

With regards to the evaluation of the complex-valued sums $S_l(k, d) = S_l^j + iS_l^y$ several methods have been proposed in the literature [24,26,27]. Those originally proposed in [24,26] display rather slow convergence properties for small values of l and all wavenumbers k and, in addition, they entail a computational cost that is proportional to $\frac{k}{p}$. While acceleration based on Kummer transforms has been advocated this is, as we have explained above, of limited applicability at higher frequencies. The recent work in [27], on the other hand, significantly improves on the convergence of the series, but the computational cost remains proportional to $\frac{k}{p}$. More precisely, for $\alpha = 0$ (the only case considered in [27]) we have $S_l = 0$ for l odd since

$$S_l(k, d) = \sum_{n \in \mathbb{Z}^*} H_l^{(1)}(k|n|d)e^{-il\varphi_n} = \sum_{n=1}^{\infty} H_l^{(1)}(k|n|d)[1 + (-1)^l].$$

The real part S_{2l}^j , on the other hand, turns out to be a finite sum given by the formula

$$S_{2l}^j(k, d) = \frac{2}{kd} + \frac{4}{d} \sum_{n=1}^{k/p} \frac{\cos(2l \arcsin(\frac{\alpha_n}{l}))}{\beta_n}$$

while the imaginary part involves an infinite series

$$S_{2l}^y(k, d) = 2\Re(\tilde{Y}_{2l}(k, d))$$

where

$$\begin{aligned} \tilde{Y}_{2l}(k, d) = & -\frac{1}{2l\pi} \sum_{n=0}^l \frac{|B_{2n}(0)|2^{(2l-1)}}{\binom{k}{p}^{2n}} + \frac{(-1)^{l+1}}{\pi} \sum_{j=1}^N \frac{\binom{k}{p}^{2l}}{\sqrt{j^2 - (\frac{k}{p})^2} [j + \sqrt{j^2 - (\frac{k}{p})^2}]^{2l}} + \\ & \frac{(-1)^{l+1} k^{2l}}{(2p)^{2l} \pi} \frac{\Gamma(2l+1)}{\Gamma(l+1/2)\Gamma(l+1)} \sum_{m=0}^{\infty} \left[\frac{\Gamma(m+l+\frac{1}{2})\Gamma(m+l+1)}{\Gamma(m+2l+1)\Gamma(m+1)} \xi_N^{\infty}(2m+2l+1) \left(\frac{k}{p}\right)^{2n} \right] \end{aligned} \quad (17)$$

for a fixed and arbitrary N , $B_n(x)$ are the Bernoulli polynomials, Γ is the gamma function, ψ is the polygamma function and

$$\xi_N^{\infty}(n) = \sum_{l=N+1}^{\infty} \frac{1}{l^n}.$$

The series in (17) converges as

$$\frac{e^{-2m \log(Np/k)}}{m^{3/2}} (= \frac{1}{m^{3/2}} (\frac{k}{Np})^{2m}) \text{ for } l \ll m$$

which is faster than the ones in [24,26] and thus provides also increased stability. Clearly, however, this formula also implies that the values of N should be chosen to significantly exceed k/p to guarantee rapid convergence [27].

5. Ewald's method: As we anticipated in §2, the application of the the Ewald method at high-frequencies requires additional considerations to guarantee stability [30]. In more detail, using [29, Eq. (7.1.23)]

$$\operatorname{erfc}(z) \sim e^{-z^2}/\sqrt{\pi z} \text{ for } |z| \gg 1$$

we have that, for large k ,

$$G_1 \sim \sum_n e^{\frac{(k^2-n^2)d^2}{4E^2} - \frac{E^2 y^2}{d^2}}. \quad (18)$$

Thus, a choice of E that is independent of frequency leads to inordinate values of the terms in the series and to inaccurate values of the $G_{\text{qp}}(x, y)$ as a result of cancellations. To avoid this difficulty, one may choose

$$E = C \frac{\sqrt{kd^2}}{\sqrt{2y}} \quad (19)$$

for some constant C independent of k (and related to the maximum allowable value for the terms in (18)). As can be easily verified, this choice (19) allows for evaluations of G_2 in (10) with a computational cost that is independent of frequency, as it puts the computational burden on the calculation of G_1 . Indeed, for the latter, we can approximate

$$G_1 \approx \frac{1}{2id} \left[\sum_{n=-N_1}^{N_1} \frac{e^{i\alpha_n x}}{\beta_n} e^{i\beta_n |y|} \operatorname{erfc}\left(\frac{i\beta_n d}{2E} + \frac{Ey}{d}\right) + \sum_{n=-N_2}^{N_2} \frac{e^{i\alpha_n x}}{\beta_n} e^{-i\beta_n |y|} \operatorname{erfc}\left(\frac{i\beta_n d}{2E} - \frac{Ey}{d}\right) \right]$$

to within an accuracy of ϵ provided

$$N_1 = \sqrt{\frac{\log(\epsilon)k}{y}} \text{ and } N_2 = \log(\epsilon)k.$$

which leads, again, to a computational complexity at least kd .

6. Integral representation: As we mentioned, the main difficulty that arises in the evaluation of the integral in (14) at high-frequencies relates to the fact that, in this case, the integrand displays large and fast oscillations which cancel out to produce a value that can be several orders of magnitude smaller than the amplitude of variations. For this reason classical quadratures tend to be unstable and unable to accurately determine the values of G_{qp} .

To substantiate this, let us consider the integral in (14) for the case $\alpha = 0$ (normal incidence) and $x = 0$; the arguments for the most general case follow largely along the same lines. In this case, we begin by noting that the integral I in (13) can be rewritten as

$$I = I_+ + I_- \quad (20)$$

where

$$I_+ = \int_0^\infty \frac{e^{iky\sqrt{u^2-2i}}}{(e^{kd(u^2-i)} - 1)\sqrt{u^2-2i}} du, \quad (21)$$

and

$$I_- = \int_0^\infty \frac{-e^{-iky\sqrt{u^2-2i}}}{(e^{kd(u^2-i)} - 1)\sqrt{u^2-2i}} du. \quad (22)$$

Using

$$\sqrt{u^2-2i} \sim 1-i \text{ for } u \sim 0,$$

we see that

$$f_+ \equiv \frac{e^{iky\sqrt{u^2-2i}}}{(e^{kd(u^2-i)} - 1)(\sqrt{u^2-2i})} \sim g_+ \equiv \frac{e^{kyu(1+i)}}{e^{kd(u^2-i)}}, \quad (23)$$

$$f_- \equiv \frac{e^{-iky\sqrt{u^2-2i}}}{(e^{kd(u^2-i)} - 1)(\sqrt{u^2-2i})} \sim g_- \equiv \frac{e^{-kyu(1+i)}}{e^{kd(u^2-i)}} \quad (24)$$

(see Figure 3) from which estimates can be derived for both the amplitude of oscillations in f_\pm as well as of their integrated values. Indeed, for instance, we have

$$\max |f_+| \sim e^{\frac{ky^2}{4d}} \gg 1, \quad |f'_+| \gg 1 \text{ and } \left| \int_0^\infty f_+ du \right| \sim \frac{1}{\sqrt{kd}} \ll 1$$

which clearly illustrates the difficulties in attempting to accurately determine the latter value in finite precision arithmetic.

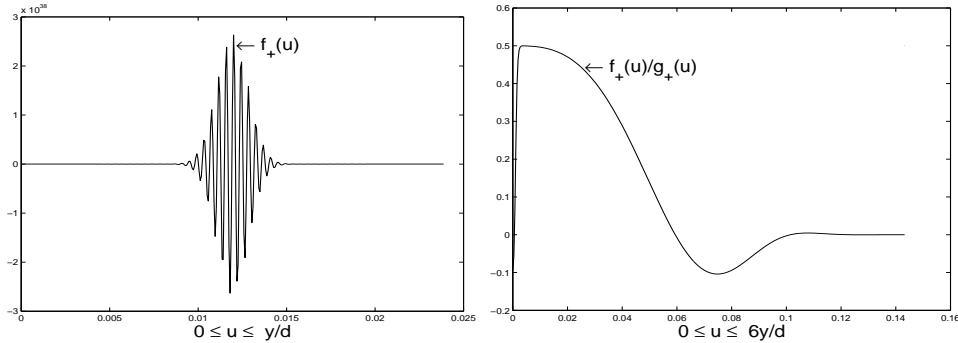


Fig. 3. The integrand f_+ in (21) and its approximation g_+ as defined in (23). Left: $\Re(f_+)$, Right: $\Re(\frac{f_+}{g_+})$, with $k = 10^5 + 0.2$, $d = 2\pi$ and $y = 0.15$.

4 A new algorithm

In this section we provide a complete derivation of our new procedure. As we anticipated, our algorithm is based on the representation (13), (20) and, more

precisely, it relies on further manipulation of the integrals in (21) and (22) in a manner so as to reduce the integration problem to one where the application of classical quadrature formulas becomes simultaneously stable and efficient. A first version of our approach is derived in §4.1. In sections 4.2 and 4.3 then we provide the details on the derivations of alternative forms of the basic scheme which, as we show, deliver progressively more effective and accurate evaluations.

4.1 The basic scheme

To begin with the derivation of our procedure, we note that, with g_+ as in (23), we have

$$\int_0^\infty f_+ du = \int_0^\infty \frac{f_+}{g_+} g_+ du$$

where the quotient f_+/g_+ is exponentially decaying and smooth save for a boundary layer (of order $(kd)^{-1/2}$) near $u = 0$. To mollify the latter we further decompose

$$\begin{aligned} \int_0^\infty f_+ du &= \int_0^\infty \frac{f_+}{g_+} g_+ du \\ &= \int_0^\infty \left[\frac{e^{iky u \sqrt{u^2 - 2i} - ky u(1+i)}}{\sqrt{u^2 - 2i}} \right] \frac{1}{(1 - e^{-kd(u^2 - i)})} g_+ du \\ &= \int_0^\infty h(u) \left(\sum_{j=0}^M \frac{1}{e^{jkd(u^2 - i)}} \right) g_+ du \\ &\quad + \int_0^\infty h(u) \frac{g_+}{e^{Mkd(u^2 - i)} - e^{(M-1)kd(u^2 - i)}} du \end{aligned} \tag{25}$$

where the function $h(u)$, given by

$$h(u) = \frac{e^{iky u \sqrt{u^2 - 2i} - ky u(1+i)}}{\sqrt{u^2 - 2i}} \tag{26}$$

displays a significantly milder transition at $u = 0$ than that of f_+/g_+ ; see Figure 4. From (25) then, we have

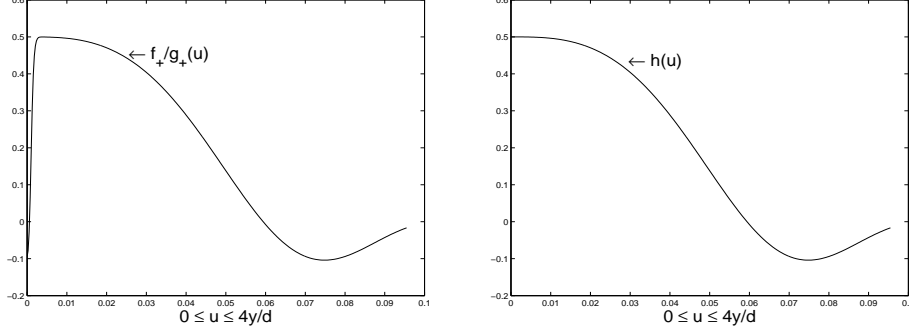


Fig. 4. Comparison of the (real parts of the) functions $f_+(u)/g_+(u)$ and $h(u)$ Left: $\Re(\frac{f_+(u)}{g_+(u)})$, Right: $\Re(h(u))$, with $k = 10^5 + 0.2$, $d = 2\pi$ and $y = 0.15$.

$$\begin{aligned}
\int_0^\infty f_+ du &= \int_0^\infty \left[\sum_{n=0}^\infty a_n u^n \right] \left(\sum_{j=0}^M \frac{1}{e^{jkd(u^2-i)}} \right) g_+ du \\
&\quad + \int_0^\infty \left(\sum_{n=0}^\infty a_n u^n \right) \frac{g_+}{e^{Mkd(u^2-i)} - e^{(M-1)kd(u^2-i)}} du \\
&= \sum_{j=1}^M \left(\sum_{n=0}^\infty a_n I_{nj} \right) + \int_0^\infty \frac{e^{iky u \sqrt{u^2-2i}}}{(e^{(M+1)kd(u^2-i)} - e^{Mkd(u^2-i)}) \sqrt{u^2-2i}} du
\end{aligned} \tag{27}$$

where

$$h(u) = \sum_{n=0}^\infty a_n u^n \tag{28}$$

and

$$I_{nj} = \int_0^\infty \frac{u^n}{e^{k(j-1)d(u^2-i)}} g_+ du = \int_0^\infty u^n \frac{e^{kyu(1+i)}}{e^{kj d(u^2-i)}} du. \tag{29}$$

The evaluation of the integrals I_{nj} in (29) is clearly preferable to that in (21), on account of the diminishing values and faster decay of the former as n and j increase. For small values of these parameters, however, a further manipulation is necessary to attain similar characteristics. In more detail, we first note that [31, Eqs. (4.146.1) and (4.146.2)] can be used to derive the identity

$$I_{0j} = \int_0^\infty \frac{e^{kyu(1+i)}}{e^{kj d(u^2-i)}} = - \int_0^\infty \frac{e^{-kyu(1+i)}}{e^{kj d(u^2-i)}} du + A_j \tag{30}$$

where

$$A_j = \sqrt{\frac{\pi}{kj d}} e^{i \frac{ky^2}{2jd}} e^{ikjd}. \tag{31}$$

From this, integrating by parts n times in both integrals in (30) we obtain the recursion

$$I_{nj} = - \int_0^\infty (-u)^n \frac{e^{-kyu(1+i)}}{e^{kj d(u^2-i)}} + A_j v_{n,j} \tag{32}$$

where

$$v_{0,j} = 1, \quad v_{1,j} = \frac{1}{w_j} \quad \text{and} \quad v_{n,j} = \frac{v_{n-1,j}}{w_j} + \frac{(n-1)v_{n-2,j}}{w_j s} \quad (33)$$

and

$$w_j = j \frac{2d}{y(1+i)}, \quad s = ky(1+i),$$

and therefore from (13) and (20)

$$\begin{aligned} G_{\text{qp}}(x, y) &= -\frac{i}{4} H_0^{(1)}(kr) - \frac{1}{\pi} (I_+ + I_-) \\ &= -\frac{i}{4} H_0^{(1)}(kr) - \frac{1}{\pi} I_- - \frac{1}{\pi} \left[\sum_{j=1}^M A_j \sum_{n=0}^{\infty} a_n v_{n,j} \right] \\ &\quad + \frac{1}{\pi} \left[\sum_{j=1}^M \int_0^{\infty} \left(\sum_{n=0}^{\infty} a_n (-u)^n \right) \frac{e^{-kyu(1+i)}}{e^{kj d(u^2-i)}} \right] \\ &\quad - \frac{1}{\pi} \int_0^{\infty} \frac{e^{iky u \sqrt{u^2-2i}}}{(e^{(M+1)kd(u^2-i)} - e^{Mkd(u^2-i)}) \sqrt{u^2-2i}} du. \end{aligned} \quad (34)$$

Even though the integrals on the right hand side of (34) can be calculated in a fast and efficient manner using classical quadratures, a further simplification can be attained using the symmetry of $h(u)$ in (26). Indeed we have

$$\sum_{n=0}^{\infty} a_n (-u)^n = h(-u) = \frac{e^{-iky u \sqrt{u^2-2i} + ky u(1+i)}}{\sqrt{u^2-2i}}, \quad (35)$$

and using this in (34) we obtain,

$$\begin{aligned} \sum_{j=1}^M \int_0^{\infty} \left(\sum_{n=0}^{\infty} a_n (-u)^n \right) \frac{e^{-kyu(1+i)}}{e^{kj d(u^2-i)}} &= \int_0^{\infty} \frac{e^{-iky u \sqrt{u^2-2i}}}{e^{kd(u^2-i)} \sqrt{u^2-2i}} du \\ &\quad - \int_0^{\infty} \frac{e^{-iky u \sqrt{u^2-2i}}}{(e^{(M+1)kd(u^2-i)} - e^{Mkd(u^2-i)}) \sqrt{u^2-2i}} du \end{aligned} \quad (36)$$

or, equivalently, from (22)

$$\begin{aligned} \sum_{j=1}^M \int_0^{\infty} \left(\sum_{n=0}^{\infty} a_n (-u)^n \right) \frac{e^{-kyu(1+i)}}{e^{kj d(u^2-i)}} \\ = I_- - \int_0^{\infty} \frac{e^{-iky u \sqrt{u^2-2i}}}{(e^{(M+1)kd(u^2-i)} - e^{Mkd(u^2-i)}) \sqrt{u^2-2i}} du. \end{aligned} \quad (37)$$

Finally, using (34) and (37), and letting

$$f_{\text{new}}^M(u) = \frac{e^{iky\sqrt{u^2-2i}} + e^{-iky\sqrt{u^2-2i}}}{(e^{(M+1)kd(u^2-i)} - e^{Mkd(u^2-i)})\sqrt{u^2-2i}} \quad (38)$$

the Green function can be rewritten as

$$G_{\text{qp}}(x, y) = -\frac{i}{4}H_0(kr) - \frac{2}{\pi}S^M - \frac{1}{\pi}I_{\text{new}}^M, \quad (39)$$

where

$$S^M = \sum_{j=1}^M A_j S_j, \quad S_j = \sum_{n=0}^{\infty} a_n v_{n,j} = \sum_{n=0}^{\infty} \frac{h^{(n)}(0)}{n!} v_{n,j} \quad (40)$$

and

$$I_{\text{new}}^M = \int_0^{\infty} f_{\text{new}}^M(u) du, \quad (41)$$

a_n are defined as in (26) and the $v_{n,j}$ are defined as in (33).

A choice of M in (40) will determine the relative computational cost between the integral I_{new}^M and the series S^M . A large value of M puts the burden on the series S while a smaller one shifts it to the integral I_{new}^M . However, at high-frequencies, a further constraint has to be taken into account relating to the large oscillations of the integrand

$$\max_{0 \leq u \leq \infty} |f_{\text{new}}^M(u)| \sim e^{\frac{ky^2}{4Md}}.$$

Clearly large variations affect negatively the stability of the evaluations and must be avoided, leading to a choice of

$$M \approx \frac{ky^2}{d}.$$

To complete the prescriptions, we must provide a rule for the truncation of the improper integral defining I_{new}^M in (41) and of the infinite series S_j in (40).

At this point we note that with this choice, the integral can be truncated to $[0, C_{\text{new}}]$ where

$$f_{\text{new}}^M(C_{\text{new}}) = \epsilon \text{ and } C_{\text{new}} = \frac{y + \sqrt{y^2 - \frac{4Md \log(\epsilon)}{k}}}{2Md} \sim \frac{1}{ky},$$

since [31, Eqs. (4.146.1) and (4.146.2)]

$$\int_{C_{\text{new}}}^{\infty} f_{\text{new}}^M(u) du \sim \epsilon \int_0^{\infty} \frac{e^{(ky-2kd)v+ikyv}}{e^{kd(v^2-i)}} dv \sim \epsilon \left[\sqrt{\frac{\pi}{4kd}} e^{(d-y)/d} e^{iky(y-2d)/(2d)} \right].$$

Also, since the integrand does not oscillate rapidly within the range $[0, C_{\text{new}}]$ (see Figure 5), a canonical quadrature can be applied to evaluate it accurately with a computational complexity independent of the wavenumber.

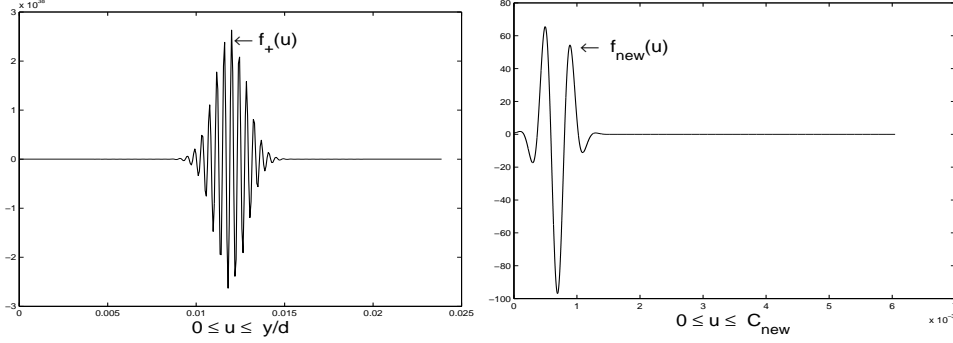


Fig. 5. The integrand original $f_+(u)$ in (23) and the new integrand $f_{\text{new}}^M(u)$ in (38). Left: $\Re(f_+)$, Right: $\Re(f_{\text{new}})$, with $k = 10^5 + 0.2$, $y = 0.15$, $d = 2\pi$ and $M = \frac{ky^2}{20d} = 17$.

Regarding the truncation of the series S_j , finally, we begin by noting that

$$h(u) = \frac{e^{iky\sqrt{u^2-2i}-kyu(1+i)}}{\sqrt{u^2-2i}} \sim e^{\frac{-ky(1-i)u^3}{4}} \text{ for } u \sim 0 \text{ and}$$

and

$$v_{n,j} \sim \frac{1}{w_j^n} \text{ for } ky \gg 1$$

so that

$$a_{3n}v_{3n,j} \sim \left(-\frac{ky(1-i)}{4w_j^3}\right)^n \frac{1}{n!} = \left(-\frac{iky^4}{(2dj)^3}\right)^n \frac{1}{n!}.$$

Using Stirling's formula then, we see that S_j must be truncated at a number $n = N$ satisfying

$$N \gtrsim 3 \frac{eky^4}{(2dj)^3}. \quad (42)$$

With these choices, it is easy to see that the computational cost of the scheme is proportional to $\frac{ky^2}{d}$, with a constant of proportionality that can be chosen not to exceed unity. Indeed, while the integrals I_{new}^M in (41) can be calculated in fixed times for any value of the wavenumber, the cost of evaluation of the series S^M in (40) does increase with increasing frequency. In more detail, from (42) we have that S_j can be truncated after $\frac{eky^4}{(2dj)^3}$ terms and this implies that the cost of evaluating S^M is

$$N_1 \frac{eky^4}{(2d)^3} + C(M - N1) \sim CM = C_1 \frac{ky^2}{d}$$

where

$$N_1 = \left(\frac{ky^4}{d^3}\right)^{1/3}.$$

As the experiments in §5 demonstrate, however, this cost is significantly lower than that of alternative methods, largely owing to quadratic dependence of the cost on the height-to-period ratio of the evaluation point. Moreover, as the results confirm, the manipulations above provide for a significant enhancement of the stability properties at high-frequencies when compared to the numerical procedures reviewed in §2. In this connection, in the next two subsections we derive alternative forms of our algorithms that, as we show, afford additional stability beyond that already attainable by the procedure described above.

4.2 Rearrangement of the series S_j : first alternative form

While, as we mentioned and as we further substantiate through numerical experiments in §5, the scheme as proposed above provides a means to evaluate the Green function that outperforms all classical procedures for small values of y/d , the extension of its favorable characteristics to larger values of this parameter necessitate some further developments. More precisely, for large values of ky^4/d^3 (cf. (42)) the terms in the series S_j in (40) become large and cancellations render its evaluation unstable, particularly for small values of j . To ameliorate this instability we appeal to the explicit formula

$$v_{n,j} = \sum_{a=0}^{\lceil \frac{n}{2} \rceil} \frac{1}{w_j^n} \frac{w_j^a}{(2s)^a} \frac{1}{a!} \prod_{i=0}^{2a-1} (n-i) \quad (43)$$

where the ceiling function is defined by

$$\lceil x \rceil = \min\{n \in \mathbb{Z} \mid x \leq n\}.$$

Substituting (43) into (40) and changing the order of summation we derive

$$\begin{aligned} S_j &= \sum_{n=0}^{\infty} a_n v_{n,j} \\ &= \sum_{n=0}^{\infty} \frac{h^{(n)}(0)}{n!} \left[\sum_{a=0}^{\lceil \frac{n}{2} \rceil} \frac{1}{w_j^n} \frac{w_j^a}{(2s)^a} \frac{1}{a!} \prod_{i=0}^{2a-1} (n-i) \right] \\ &= \sum_{a=0}^{\infty} \frac{w_j^a}{(2s)^a} \frac{1}{a!} \sum_{n \geq 2a}^{\infty} \frac{h^{(n)}(0)}{n!} \frac{1}{w_j^n} \prod_{i=0}^{2a-1} (n-i). \end{aligned}$$

Noting that the inner sum can be explicitly evaluated

$$\sum_{n \geq 2a}^{\infty} \frac{h^{(n)}(0)}{n!} \frac{1}{w_j^n} \prod_{i=0}^{2a-1} (n-i) = h^{(2a)}\left(\frac{1}{w_j}\right)$$

and letting

$$h_w(u) \equiv h\left(\frac{u}{w_j}\right) = \frac{e^{\frac{iky u}{w_j} \sqrt{\frac{u^2}{w_j^2} - 2i} - \frac{ky u(1+i)}{w_j}}}{\sqrt{\frac{u^2}{w_j^2} - 2i}} \quad (44)$$

we obtain that S_j can be rewritten as

$$S_j = \sum_{a=0}^{\infty} \frac{h_w^{(2a)}(1)}{a!} \frac{w_j^a}{(2s)^a}. \quad (45)$$

The advantage of (45) over (40) lies upon the significantly smaller variations of the function $h_w(u)$ when compared to those of $h(u)$, which results in the derivatives of the former being substantially smaller in magnitude; see Figure 6.

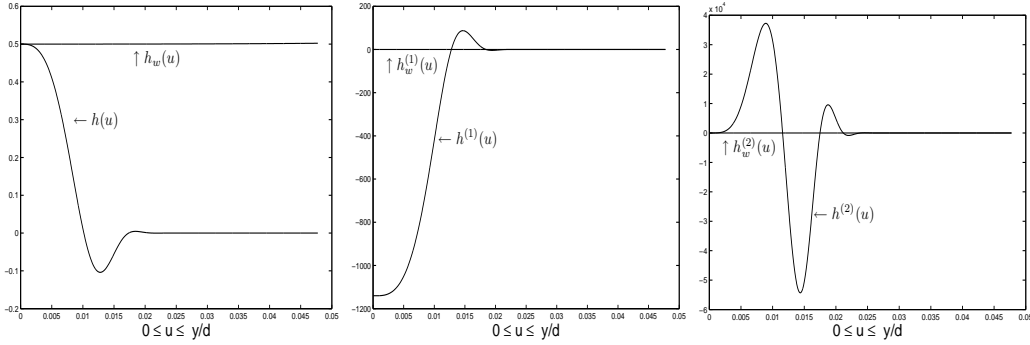


Fig. 6. Comparison of the (real parts of the) derivatives of the functions $h(u)$ and $h_w(u)$ that enter the evaluation of the sums S_j in (40) and (45), respectively, for $k = 10^7 + 0.2$ and $y = 0.3$.

The derivatives of the function $h_w(u)$ in (45) can be calculated using Leibniz's rule and suitable recursions. In detail,

$$h_w(u) = \frac{e^{\frac{iky u}{w_j} \sqrt{\frac{u^2}{w_j^2} - 2i} - \frac{ky u(1+i)}{w_j}}}{\sqrt{\frac{u^2}{w_j^2} - 2i}} = f(u)e^{g(u)} \quad (46)$$

where

$$f(u) = \frac{1}{\sqrt{\frac{u^2}{w_j^2} - 2i}} \quad \text{and} \quad g(u) = \frac{iky u}{w_j} \sqrt{\frac{u^2}{w_j^2} - 2i} - \frac{ky u(1+i)}{w_j}.$$

Using Leibniz's rule we have

$$h_w^{(2a)}(u) = \sum_{b=0}^{2a} \binom{2a}{b} f^{(b)}(u) (e^{g(u)})^{(2a-b)} \quad (47)$$

where

$$f^{(1)}(1) = -\frac{1}{\left(\frac{1}{w_j^2} - 2i\right)^{3/2}},$$

$$f^{(n)}(1) = -\frac{(2n-1)f^{(n-1)}(1)}{\left(\frac{1}{w_j^2} - 2i\right)^{3/2}} - \frac{(n-1)^2 f^{(n-2)}(1)}{\left(\frac{1}{w_j^2} - 2i\right)^{3/2}}$$

and

$$D^n(e^{g(u)})\Big|_{u=1} = \sum_{j=1}^n \binom{n-1}{j-1} g^{(j)}(1) D^{n-j}(e^{g(u)})\Big|_{u=1} \quad (48)$$

with $g^{(n)}(1)$ given recursively by

$$g^{(n)}(1) = -\frac{(2n-3)g^{(n-1)}(1)}{\left(\frac{1}{w_j^2} - 2i\right)^{1/2} w_j^2} - \frac{n(n-4)g^{(n-2)}(1)}{\left(\frac{1}{w_j^2} - 2i\right)^{1/2} w_j^2}. \quad (49)$$

Finally, to decide on the truncation parameter for the sum in (45) we note that, as can be readily verified, for $ky \gg 1$ we have

$$h_w^{(2a)}(1) \sim \left[-\frac{3(1-i)ky}{4w_j^3} \right]^{2a} h_w(1)$$

and thus

$$\frac{h_w^{(2a)}(1)}{a!} \frac{w_j^a}{(2s)^a} \sim \left(\frac{9ky^6}{128j^5 d^5} \right)^a \frac{1}{a!}$$

which implies that S_j must be truncated at a number N such that

$$N \gtrsim \frac{9eky^6}{128(jd)^5}; \quad (50)$$

compare with (42).

4.3 A further rearrangement of the series S_j : second alternative form

As we have explained, the rearrangement in (45) provides enhanced stability to the evaluation of the series S_j in (40) for large values of ky^4/d^3 . In fact, as can be readily seen, this new form allows for the accurate evaluation of the series for large values of this parameter provided it does not significantly exceed the ratio $(d/y)^2$. If, on the other hand, $ky^6/d^5 \gg 1$ a further rearrangement is necessary. We note here that, similarly, subsequent rearrangements may be possible, that allow for the extension of the stable characteristics of the evaluation to bounded values of $ky^{2\ell}/d^{2\ell-1}$.

To enable the next rearrangement, we proceed as in §4.2 by first deriving an explicit formula for the series in (45) that does not rely on the recurrences

(48) and (49). More precisely, appealing to Faà di Bruno's formula [32], we have

$$D^n e^{g(u)} = e^{g(u)} \sum_{\tilde{m}} \frac{n!}{m_1! m_2! \cdots m_n!} \left(\frac{g'(u)}{1!}\right)^{m_1} \left(\frac{g''(u)}{2!}\right)^{m_2} \cdots \left(\frac{g^{(n)}(u)}{n!}\right)^{m_n} \quad (51)$$

where the sum is over all partitions $\tilde{m} = (m_1, m_2, \dots, m_n)$ of n such that $n = m_1 + 2m_2 + \cdots + nm_n$. Using (47) in (45), exchanging the order of summation, and substituting (51) we obtain

$$\begin{aligned} S_j &= \sum_{a=0}^{\infty} \frac{h_w^{(2a)}(1)}{a!} \frac{w_j^a}{(2s)^a} \\ &= \sum_{a=0}^{\infty} \sum_{b=0}^{2a} \left[\binom{2a}{b} f^{(b)}(1) D^{2a-b}(e^{g(u)}) \Big|_{u=1} \frac{w_j^a}{a!(2s)^a} \right] \\ &= \sum_{b=0}^{\infty} f^{(b)}(1) \sum_{a=0}^{\infty} \left[\binom{2a}{b} D^{2a-b}(e^{g(u)}) \Big|_{u=1} \frac{w_j^a}{a!(2s)^a} \right] \\ &= \sum_{b=0}^{\infty} f^{(b)}(1) \sum_{a=0}^{\infty} \left[\binom{2a}{b} e^{g(1)} \right. \\ &\quad \left. \times \sum_{\tilde{m}} \left[\frac{(2a-b)!}{m_1! m_2! \cdots m_{(2a-b)}!} \left(\frac{g'(1)}{1!}\right)^{m_1} \cdots \left(\frac{g^{(2a-b)}(1)}{(2a-b)!}\right)^{m_{(2a-b)}} \frac{w_j^a}{a!(2s)^a} \right] \right] \\ &= \sum_{b=0}^{\infty} f^{(b)}(1) S_{j,b} \end{aligned}$$

where

$$\begin{aligned} S_{j,b} &= \sum_{a=0}^{\infty} \left[\binom{2a}{b} e^{g(1)} \right. \\ &\quad \left. \times \sum_{\tilde{m}} \left[\frac{(2a-b)!}{m_1! m_2! \cdots m_{(2a-b)}!} \left(\frac{g'(1)}{1!}\right)^{m_1} \cdots \left(\frac{g^{(2a-b)}(1)}{(2a-b)!}\right)^{m_{(2a-b)}} \frac{w_j^a}{a!(2s)^a} \right] \right]. \end{aligned} \quad (52)$$

and the sum is over all partitions $\tilde{m} = (m_1, m_2, \dots, m_n)$ of $2a - b$ such that $2a - b = m_1 + 2m_2 + \cdots + (2a - b)m_{2a-b}$.

The evaluation of the series $S_{j,b}$ in (52) can become unstable on account of the high-order derivatives of the exponential in (46). The most extreme case corresponds to $b = 0$ where each term in the series entails a derivative of order

2a. In this case, exchanging the order of summation over a and m_1 , we have

$$\begin{aligned}
S_{j,0} &= \sum_{a=0}^{\infty} e^{g(1)} \sum_{\tilde{m}} \left[\frac{(2a)!}{m_1! m_2! \cdots m_{(2a)}!} \left(\frac{g'(1)}{1!}\right)^{m_1} \cdots \left(\frac{g^{(2a)}(1)}{(2a)!}\right)^{m_{(2a)}} \frac{w_j^a}{a!(2s)^a} \right] \\
&= \sum_{a=0}^{\infty} \sum_{c=0}^{2a} \sum_{\tilde{c}} \left[\frac{(2a)!}{(2a-c)! m_2! \cdots m_c!} \left(\frac{g'(1)}{1!}\right)^{(2a-c)} \cdots \left(\frac{g^{(c)}(1)}{c!}\right)^{m_c} \frac{w_j^a}{a!(2s)^a} \right] \\
&= \sum_{c=0}^{\infty} \sum_{a=\lceil \frac{c}{2} \rceil}^{\infty} \sum_{\tilde{c}} \left[\frac{(2a)!}{(2a-c)! m_2! \cdots m_c!} \left(\frac{g'(1)}{1!}\right)^{(2a-c)} \cdots \left(\frac{g^{(c)}(1)}{c!}\right)^{m_c} \frac{w_j^a}{a!(2s)^a} \right] \\
&= e^{g(1)} \sum_{c=0}^{\infty} \sum_{\tilde{c}} \left[\left(\frac{g''(1)}{2!}\right)^{m_2} \left(\frac{g'''(1)}{3!}\right)^{m_3} \cdots \left(\frac{g^{(c)}(1)}{c!}\right)^{m_c} \right] \sum_{a=\lceil \frac{c}{2} \rceil}^{\infty} \left[\frac{(2a)!}{(2a-c)!} \left(\frac{g'(1)}{1!}\right)^{(2a-c)} \frac{w_j^a}{a!(2s)^a} \right]
\end{aligned}$$

where the sum is over all partitions $\tilde{c} = (m_2, m_3, \dots, m_c)$ of c such that $c = 2m_2 + 3m_3 + 4m_4 + \cdots + cm_c$. Using the relation

$$\frac{(2a)!}{(2a-c)! a!} = 2^{\lceil \frac{c}{2} \rceil} \frac{\prod_{j=0}^{\lceil \frac{c}{2} \rceil - 1} (2a - 2j - 1)}{(a - \lceil \frac{c}{2} \rceil)!}$$

we further have

$$\begin{aligned}
S_{j,0} &= e^{g(1)} \sum_{c=0}^{\infty} \sum_{\tilde{c}} \left(\frac{g''(1)}{2!}\right)^{m_2} \left(\frac{g'''(1)}{3!}\right)^{m_3} \cdots \left(\frac{g^{(c)}(1)}{c!}\right)^{m_c} \\
&\quad \times \sum_{a=\lceil \frac{c}{2} \rceil}^{\infty} \left[\frac{2^{\lceil \frac{c}{2} \rceil} \prod_{j=0}^{\lceil \frac{c}{2} \rceil - 1} (2a - 2j - 1)}{(a - \lceil \frac{c}{2} \rceil)!} \left(\frac{g'(1)}{1!}\right)^{(2a-c)} \frac{w_j^a}{(2s)^a} \right] \\
&= e^{g(1)} \sum_{c=0}^{\infty} \sum_{\tilde{c}} \left(\frac{g''(1)}{2!}\right)^{m_2} \left(\frac{g'''(1)}{3!}\right)^{m_3} \cdots \left(\frac{g^{(c)}(1)}{c!}\right)^{m_c} \frac{(2w_j)^{\lceil \frac{c}{2} \rceil}}{(2s)^{\lceil \frac{c}{2} \rceil}} (g'(1))^{2\lceil \frac{c}{2} \rceil - c} \\
&\quad \times \sum_{i=0}^{\infty} \left[\frac{\prod_{j=0}^{\lceil \frac{c}{2} \rceil - 1} (2a + 2\lceil \frac{c}{2} \rceil - 2j - 1)}{i!} \left(\frac{g'(1)}{1!}\right)^{(2i)} \frac{w_j^i}{(2s)^i} \right]
\end{aligned} \tag{53}$$

where the floor function defined by $\lfloor x \rfloor = \max\{n \in \mathbb{Z} \mid x \leq n\}$. This latter form allows, as before, for some *explicit* evaluations in terms of a function $\tilde{h}_w(u)$ defined as

$$\tilde{h}_w(u) = \sum_{a=0}^{\infty} (g'(1))^{2a} \frac{w_j^a}{a!(2s)^a} u^a = e^{[g'(1)]^2 \frac{w_j}{2s} u}. \tag{54}$$

Specifically, from (53) we have

$$S_{j,0} = e^{g(1)} \sum_{c=0}^{\infty} \sum_{\tilde{c}} \left(\left(\frac{g''(1)}{2!} \right)_{m_2} \left(\frac{g'''(1)}{3!} \right)_{m_3} \dots \left(\frac{g^{(c)}(1)}{c!} \right)_{m_c} (g'(1))^{2\lceil \frac{c}{2} \rceil - c} \left(\frac{2w_j}{2s} \right)^{\lceil \frac{c}{2} \rceil} \right) \times \left[\sum_{j=0}^c a_{cj} \tilde{h}_w^{(j)}(1) \right] \quad (55)$$

where the coefficients a_{ij} satisfy

$$\prod_{j=0}^{\lfloor \frac{c}{2} \rfloor - 1} (2a + 2\lceil \frac{c}{2} \rceil - 2j - 1) = \sum_{i=0}^{\lfloor \frac{c}{2} \rfloor} a_{ci} \prod_{n=0}^{i-1} (a - n).$$

Again, as in the case of the first rearrangement of §4.2, the benefits of using the representation in (55) over that in (45) stem from a substantial decrease in the magnitude of the variations of the newly defined function $\tilde{h}_w(u)$ in (54) when compared to those of the previously function h_w (cf. (44)) entering (45); see Figure 7. This, in turn, further accelerates the convergence of the series which can now be truncated

$$N \gtrsim \frac{27eky^8}{2^8(jd)^7};$$

compare with (42) and (50).

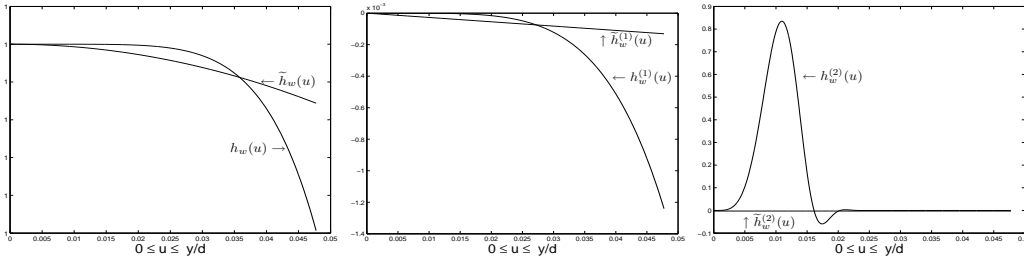


Fig. 7. Comparison of the (real parts of the) derivatives of the functions $h_w(u)$ in (44) and $\tilde{h}_w(u)$ in (54) that enter the evaluation of the sums S_j in (45) and (55), respectively, for $k = 10^7 + 0.2$ and $y = 0.3$.

5 Numerical results

In this section, we present the results of a variety of numerical experiments that compare the performance of our new schemes with the classical procedures reviewed in §2. Specifically, we compare the results obtainable through the three different versions of our algorithm, corresponding to evaluations of the

series S_j through (40), (45) or (55), with the classical spectral representation, Kummer and Ewald’s transforms and the more recent lattice sums method; the spatial and integral representations are excluded due to their very poor convergence properties, as discussed above.

The implementation of every scheme is largely straightforward, as it entails evaluations of standard special functions and simple sums and products. In the case of our new schemes, as well as in the implementation of Ewald summation, quadrature rules are additionally needed. For the Ewald method we follow the suggestions in [14] and use an adaptive Simpson’s rule (the necessary evaluations of the complementary error function – for complex arguments – are performed using the algorithm in [33]). The methods introduced above, on the other hand, rely on the evaluation of integrals (cf. I_{new}^M in (41)) with integrands that display exponentially small (odd order) derivatives at the boundary of the integration domain and are thus amenable to very accurate evaluations via the trapezoidal rule.

A difficulty does arise for every method relating to the evaluation in finite precision arithmetic of highly oscillatory functions as the frequency increases, due to the large relative errors in their values that might result from small relative errors in their phases. For instance, the evaluation of the quantity

$$E_j = e^{ijkd} \tag{56}$$

for large values of k becomes inexact as the calculation of

$$k_{mp} = \text{mod} \left(\frac{k}{p}, 1 \right) = \text{mod} \left(\frac{d}{2\pi} k, 1 \right) \tag{57}$$

gets progressively more inaccurate with increasing frequency. Interestingly, in this connection, our schemes display an additional advantage over the alternative procedures as they allow for enhanced accuracy through the multi-precision evaluation of *only* a few quantities. In the simplest case, the *single* quantity (57) can be evaluated in multi-precision (with a number of additional digits that grows only logarithmically with frequency), and inserted in (31) and (38) when computing the value of E_j in (56). In the experiments that follow

$$k = 10^n + 0.2 \text{ for } n \in \mathbb{N} \tag{58}$$

and the period is taken to be $d = 2\pi$ so that

$$k_{mp} = \text{mod} \left(\frac{k}{p}, 1 \right) = 0.2$$

and double precision accuracy for E_j can be readily attained.

In Tables 1– 12, we present four specific sets of experiments (performed in double precision arithmetic) designed to provide a comprehensive assessment

of the performance of the different schemes. The first set of results, in Tables 1– 4, illustrate the behavior as the height y of the evaluation point is increased; results for $x = 0$ and $y = 0.01, 0.1, 0.3$ and $y = 0.5$ are displayed for wavenumbers as in (58) with $4 \leq n \leq 8$ under normal incidence ($\alpha = 0$). The second set of results, in Tables 5– 8, show similar experiments but with heights that depend on the wavenumber, namely $y/d = 2(kd)^{-1/(2n)}$ for $2 \leq n \leq 5$. The third and fourth sets (Tables 9– 10 and 11– 12, respectively) show that all methods perform similarly for evaluation points that are horizontally displaced ($x = \frac{d}{2}$), and also under oblique incidence ($\alpha = k \sin(\frac{\pi}{4})$). The only difference here is an increase in computational times across the board that results from the loss of symmetry in the formulas (which is exploited in the evaluations of Tables 1– 8).

Each table displays the relative error and computational time (t) for seven numerical procedures: the spectral representation (“Spe.”), Kummer acceleration (“Kum.”), Ewald summation (“Ewa.”), the lattice sums method (“LSM”), and the three variants of the schemes introduced in §4, labeled NA_1 (which uses (40)), NA_2 (which relies on the first rearrangement (45)) and NA_3 (based on (55)). For the evaluation of the relative error

$$\text{err} = \frac{|G_{\text{qp}}^{\text{Exact}}(k, x, y) - G_{\text{qp}}^{\text{Method}}(k, x, y)|}{|G_{\text{qp}}^{\text{Exact}}(k, x, y)|} \quad (59)$$

an “exact solution” $G_{\text{qp}}^{\text{Exact}}(k, x, y)$ was computed in quadruple precision arithmetic (using the spectral representation to avoid biases).

The tables confirm the expected behavior of each methodology, as discussed above. The spectral representation, for instance, displays a stable behavior, hindered only by the large phase errors that result from the evaluation of trigonometric functions at large values of the argument (as in (56)), and which result in a (slow) progressive loss of accuracy as the frequency increases. The Kummer transformation, on the other hand, displays a stronger instability, enhanced with increasing $|y|$, as the values of the wavenumber exceed the ratio $1/\sqrt{|y|d}$ (cf. (15)). The use of the Ewald transformation, in turn, leads to results that are comparable to those attainable by the spectral summation in terms of precision; the corresponding computational times, however, are significantly larger, mainly due to the need for repeated evaluation of the complementary error (as we explained, the actual number of terms necessary for accurate calculations based on the Ewald procedure with the choice (19) is comparable to that needed in the spectral sums). For the lattice sums method, finally, we again find that the accuracy is comparable to that of the spectral representation. As for timings, we only report here the times corresponding to evaluation of the series (7) *assuming* that the values of the lattice sums S_l defined by (8) have been pre-computed. Even though this latter evaluations can be done once and re-used to calculate the Green’s function at any point,

the timings they involve grow quadratically with wavenumber and can thus quickly become prohibitive as the frequency increases. The results for LSM in Tables 1–4 are therefore fully computed only for the lower values of k , where run times (including the lattice sum evaluations) remain in the order of hours; on the other hand, and for illustrative purposes, for higher values of k (for which the evaluation of S_l would entail times on the order of days or months), the times correspond to the evaluation of the series (7) with arbitrarily chosen coefficients. Note that even this reduced times are significantly higher than those incurred by alternative techniques, largely due to the expense associated with the accurate calculation of Bessel functions.

Finally, the schemes introduced here can be seen to consistently outperform the alternative procedures. As the tables show, for smaller values of the height $|y|$ the evaluation through the initial implementation NA_1 is sufficient to efficiently provide accurate answers (see e.g. Tables 1, 2, 5, 6, 11 and 12). As the height increases, however, the accuracy deteriorates and the rearrangements of §4.2 and §4.3 become necessary to restore stability. As shown in Tables 3, 4, and 7–10, with these modifications the new approach can be used to significantly accelerate the evaluation of the Green function while, at the same time, providing a substantial expansion of the domain wherein this can be performed in a stable manner.

Table 1

Error (59) and computational times (t) for evaluation of $G_{qp}(x, y)$ with $\alpha = 0, k = 10^n + 0.2, y = 0.01, x = 0$.

n	Spe.	t	Kum.	t	LSM	t	Ewa.	t	NA_1	t	NA_2	t	NA_3	t
4	5e-13	0.01s	3e-08	0.02s	4e-13	0.02	5e-13	0.6s	2e-14	0.02s	2e-14	0.02s	2e-14	0.02s
5	3e-12	0.08s	3e-05	0.1s	4e-12	0.06	3e-12	3s	2e-12	0.02s	2e-12	0.02s	2e-12	0.02s
6	7e-11	0.8s	8e-02	1s	9e-11	0.5s	7e-11	30s	3e-12	0.02s	3e-12	0.02s	3e-12	0.02s
7	2e-09	8s	2e+00	10s	...	5s	2e-09	314s	7e-12	0.02s	7e-12	0.02s	7e-12	0.02s
8	2e-08	82s	7e+02	105s	...	53s	2e-08	43m	9e-11	0.02s	9e-11	0.02s	9e-11	0.05s

Table 2

Error (59) and computational times (t) for evaluation of $G_{qp}(x, y)$ with $\alpha = 0, k = 10^n + 0.2, y = 0.1, x = 0$.

n	Spe.	t	Kum.	t	LSM	t	Ewa.	t	NA_1	t	NA_2	t	NA_3	t
4	5e-12	0.01s	7e-07	0.02s	4e-12	0.05s	5e-12	0.7s	1e-14	0.02s	1e-14	0.02s	1e-14	0.02s
5	7e-11	0.08s	1e-03	0.1s	1e-10	0.5s	7e-11	3s	5e-13	0.02s	5e-13	0.02s	5e-13	0.02s
6	2e-09	0.8s	6e-01	1s	...	5s	2e-09	31s	4e-12	0.02s	4e-12	0.02s	4e-12	0.03s
7	9e-08	8s	2e-01	10s	...	55s	9e-08	304s	2e-11	0.03s	2e-11	0.5s	2e-11	0.04s
8	5e-07	139s	2e+03	142s	...	524s	5e-07	43m	1e-09	0.08s	1e-09	0.2s	1e-09	0.3s

Table 3

Error (59) and computational times (t) for evaluation of $G_{\text{qp}}(x, y)$ with $\alpha = 0, k = 10^n + 0.2, y = 0.3, x = 0$.

n	Spe.	t	Kum.	t	LSM	t	Ewa.	t	NA ₁	t	NA ₂	t	NA ₃	t
4	3e-11	0.01s	2e-06	0.02s	3e-11	0.2s	3e-11	0.6s	4e-14	0.02s	4e-14	0.02s	3e-14	0.02s
5	3e-10	0.08s	2e-03	0.1s	6e-10	1.5s	3e-10	3.5s	1e-12	0.02s	1e-12	0.02s	1e-12	0.08s
6	7e-09	0.8s	3e-01	1s	...	15s	7e-09	30s	1e-02	0.03s	1e-12	0.04s	1e-12	0.08s
7	2e-07	13s	3e+00	13s	...	157s	2e-07	320s	2e+15	0.08s	2e-10	0.2s	2e-10	0.2s
8	3e-06	141s	1e+03	144s	...	1572s	3e-06	43m	7e+48	0.5s	3e-09	2s	1e-09	2.5s

Table 4

Error (59) and computational times (t) for evaluation of $G_{\text{qp}}(x, y)$ with $\alpha = 0, k = 10^n + 0.2, y = 0.5, x = 0$.

n	Spe.	t	Kum.	t	LSM	t	Ewa.	t	NA ₁	t	NA ₂	t	NA ₃	t
4	9e-11	0.01s	3e+00	0.02s	7e-11	0.3s	9e-11	0.6s	4e-13	0.02s	4e-13	0.02s	4e-13	0.06s
5	8e-10	0.08s	2e+00	0.1s	1e-09	2.6s	8e-10	3.5s	5e-13	0.02s	8e-13	0.02s	1e-12	0.06s
6	1e-08	0.8s	7e-01	1s	...	26s	1e-18	30s	6e+11	0.04s	2e-11	0.09s	2e-11	0.1s
7	1e-06	14s	2e+01	15s	...	263s	1e-06	323s	2e+45	0.2s	5e-06	0.6s	4e-08	0.7s
8	1e-06	142s	4e+02	155s	...	50m	1e-06	43m	5e+77	1.5s	2e+02	5.6s	4e-04	7s

Table 5

Error (59) and computational times (t) for evaluation of $G_{\text{qp}}(x, y)$ with $\alpha = 0, k = 10^n + 0.2, y = 2k^{-\frac{1}{4}}, x = 0$.

n	Spe.	t	Kum.	t	Ewa.	t	NA ₁	t	NA ₂	t	NA ₃	t
4	1e-11	0.01s	4e-07	0.02s	1e-11	0.7s	8e-14	0.02s	9e-14	0.02s	8e-14	0.02s
5	1e-10	0.08s	7e-04	0.1s	1e-10	3.6s	1e-12	0.02s	1e-12	0.02s	1e-12	0.02s
6	1e-09	0.8s	8e-01	1s	1e-09	32s	2e-12	0.02s	2e-12	0.02s	2e-12	0.02s
7	1e-08	8s	2e+00	10s	1e-08	306s	3e-11	0.02s	3e-11	0.03s	3e-11	0.02s
8	8e-08	117s	8e+02	118s	8e-08	43m	3e-11	0.02s	3e-11	0.05s	3e-11	0.05s

Appendix A: Formulation of the new algorithm for arbitrary incidence and evaluation points

In this appendix we provide the details on the extension of the formulas (39)–(41) to the case of general horizontal displacement x and general incidence α . We begin by noting that, in this most general case, formulas (13) and (20)

Table 6

Error (59) and computational times (t) for evaluation of $G_{\text{qp}}(x, y)$ with $\alpha = 0, k = 10^n + 0.2, y = 2k^{-\frac{1}{6}}, x = 0$.

n	Spe.	t	Kum.	t	Ewa.	t	NA ₁	t	NA ₂	t	NA ₃	t
4	4e-11	0.01s	6e-06	0.02s	4e-11	0.7s	6e-13	0.02s	6e-13	0.02s	6e-13	0.02s
5	2e-10	0.1s	5e-04	0.1s	2e-10	3s	5e-13	0.02s	5e-13	0.02s	5e-13	0.02s
6	3e-08	1s	2e+00	1s	3e-08	31s	3e-11	0.02s	3e-11	0.03s	3e-11	0.02s
7	2e-07	8s	7e+00	10s	2e-07	305s	3e-10	0.03s	3e-10	0.07	3e-10	0.05s
8	4e-07	144s	2e+02	151s	4e-07	43m	2e-09	0.07s	2e-09	0.2s	2e-09	0.08s

Table 7

Error (59) and computational times (t) for evaluation of $G_{\text{qp}}(x, y)$ with $\alpha = 0, k = 10^n + 0.2, y = 2k^{-\frac{1}{8}}, x = 0$.

n	Spe.	t	Kum.	t	Ewa.	t	NA ₁	t	NA ₂	t	NA ₃	t
4	4e-11	0.01s	4e-06	0.02s	4e-11	0.6s	3e-13	0.02s	4e-13	0.02s	4e-13	0.04s
5	9e-10	0.1s	2e-03	0.1s	9e-10	3s	1e-12	0.02s	1e-12	0.02s	1e-12	0.04s
6	3e-08	0.9s	2e+00	1s	3e-08	30s	2e-08	0.03s	6e-12	0.05s	5e-12	0.05s
7	2e-07	13s	7e+00	14s	2e-07	318s	4e+08	0.06s	1e-10	0.2s	1e-10	0.2s
8	8e-07	146s	1e+03	152s	8e-07	43m	3e+25	0.3s	1e-10	1s	1e-10	1s

Table 8

Error (59) and computational times (t) for evaluation of $G_{\text{qp}}(x, y)$ with $\alpha = 0, k = 10^n + 0.2, y = 2k^{-\frac{1}{10}}, x = 0$.

n	Spe.	t	Kum.	t	Ewa.	t	NA ₁	t	NA ₂	t	NA ₃	t
4	6e-11	0.01s	2e-04	0.02s	6e-11	0.7s	3e-14	0.02s	8e-14	0.02s	2e-11	0.05s
5	1e-09	0.08s	7e-03	0.1s	1e-09	3s	1e-08	0.02s	4e-12	0.03s	3e-11	0.05s
6	9e-09	0.8s	6e-02	1s	9e-09	31s	7e+11	0.04s	3e-11	0.09s	4e-11	0.1s
7	8e-07	14s	5e+00	15s	8e-07	324s	2e+32	0.1s	4e-10	0.5s	4e-10	0.5s
8	3e-06	147s	1e+03	152s	3e-06	43m	1e+52	0.6s	3e-07	2s	3e-07	3s

take on the form

$$G_{\text{qp}}(x, y) = -\frac{i}{4}H_0^{(1)}(kr) - \frac{1}{2\pi}(I_+^1 + I_-^1 + I_+^2 + I_-^2)$$

Table 9

Error (59) and computational times (t) for evaluation of $G_{\text{qp}}(x, y)$ with $\alpha = 0, k = 10^n + 0.2, y = 0.1, x = \frac{d}{2}$.

n	Spe.	t	NA ₁	t	NA ₂	t	NA ₃	t
4	4e-11	0.01s	1e-12	0.04s	1e-12	0.04s	1e-12	0.04s
5	2e-10	0.07s	2e-12	0.04s	2e-12	0.04s	2e-12	0.04s
6	4e-09	1.1s	4e-11	0.05s	4e-11	0.05s	4e-11	0.05s
7	2e-07	13s	2e-07	0.08s	1e-09	0.1s	1e-09	0.1s
8	6e-06	136s	1e+16	0.4s	5e-08	0.8s	5e-08	0.8s

Table 10

Error (59) and computational times (t) for evaluation of $G_{\text{qp}}(x, y)$ with $\alpha = 0, k = 10^n + 0.2, y = 2k^{-\frac{1}{6}}, x = \frac{d}{2}$.

n	Spe.	t	NA ₁	t	NA ₂	t	NA ₃	t
4	2e-10	0.01s	4e-12	0.04s	6e-11	0.04s	6e-11	0.04s
5	6e-10	0.07s	4e-09	0.04s	5e-12	0.04s	5e-12	0.04s
6	5e-09	1.1s	2e-04	0.05s	2e-11	0.07s	2e-11	0.07s
7	9e-08	13s	4e+02	0.1s	5e-10	0.2s	5e-10	0.2s
8	3e-07	135s	5e+10	0.3s	4e-09	0.7s	4e-09	0.7s

Table 11

Error (59) and computational times (t) for evaluation of $G_{\text{qp}}(x, y)$ with $\alpha = k \sin(\frac{\pi}{4}), k = 10^n + 0.2, y = 0.1, x = 0$.

n	Spe.	t	NA ₁	t	NA ₂	t	NA ₃	t
4	4e-11	0.02s	1e-11	0.04s	1e-11	0.04s	1e-11	0.04s
5	1e-09	0.16s	1e-09	0.05s	1e-09	0.05s	1e-09	0.05s
6	1e-08	1.5s	2e-09	0.06s	2e-09	0.07s	2e-09	0.07s
7	2e-07	15s	7e-08	0.1s	7e-08	0.15s	7e-08	0.15s
8	4e-07	281s	2e-06	0.6s	2e-06	1s	2e-06	1s

where

$$\begin{aligned}
I_+^1 &= \int_0^\infty \frac{e^{iky\sqrt{u^2-2i}+kx(u^2-i)}}{(e^{-iad}e^{kd(u^2-i)} - 1)\sqrt{u^2-2i}} du, \\
I_-^1 &= \int_0^\infty \frac{e^{-iky\sqrt{u^2-2i}+kx(u^2-i)}}{(e^{-iad}e^{kd(u^2-i)} - 1)\sqrt{u^2-2i}} du, \\
I_+^2 &= \int_0^\infty \frac{e^{iky\sqrt{u^2-2i}-kx(u^2-i)}}{(e^{iad}e^{kd(u^2-i)} - 1)\sqrt{u^2-2i}} du, \\
I_-^2 &= \int_0^\infty \frac{e^{-iky\sqrt{u^2-2i}-kx(u^2-i)}}{(e^{iad}e^{kd(u^2-i)} - 1)\sqrt{u^2-2i}} du.
\end{aligned}$$

Table 12

Error (59) and computational times (t) for evaluation of $G_{\text{qp}}(x, y)$ with $\alpha = k \sin(\frac{\pi}{4})$, $k = 10^n + 0.2$, $y = 2k^{-\frac{1}{6}}$, $x = 0$.

n	Spe.	t	NA ₁	t	NA ₂	t	NA ₃	t
4	7e-12	0.02s	1e-12	0.04s	1e-12	0.04s	1e-12	0.04s
5	3e-09	0.16s	2e-09	0.05s	2e-09	0.06s	2e-09	0.06s
6	1e-08	1.5s	2e-09	0.08s	2e-09	0.09s	2e-09	0.09s
7	3e-07	15s	3e-08	0.15s	3e-08	0.2s	3e-08	0.2s
8	2e-07	275s	1e-06	0.5s	1e-06	0.9s	1e-06	0.9s

Note that for $\alpha = 0$ and $x = 0$, we have $I_{\pm}^1 = I_{\pm}^2$.

As in (25) and (27), to deal with I_{+}^a for $a = 1, 2$, we let

$$f_{+}^a = \frac{e^{iky u \sqrt{u^2 - 2i} + (3-2a)kx(u^2 - i)}}{(e^{(2a-3)i\alpha d} e^{kd(u^2 - i)} - 1)\sqrt{u^2 - 2i}} \quad \text{and} \quad f_{-}^a = \frac{e^{-iky u \sqrt{u^2 - 2i} + (3-2a)kx(u^2 - i)}}{(e^{(2a-3)i\alpha d} e^{kd(u^2 - i)} - 1)\sqrt{u^2 - 2i}},$$

and proceed as in §4.1, to derive

$$\begin{aligned} I_{+}^a &= \int_0^{\infty} f_{+}^a du \\ &= \int_0^{\infty} \frac{e^{iky u \sqrt{u^2 - 2i} + (3-2a)kx(u^2 - i)}}{\sqrt{u^2 - 2i}} \left(\sum_{j=1}^M \frac{1}{e^{(2a-3)i\alpha j d} e^{kdj(u^2 - i)}} \right. \\ &\quad \left. + \frac{1}{(e^{(2a-3)i\alpha(M+1)d} e^{k(M+1)d(u^2 - i)} - e^{(2a-3)i\alpha M d} e^{kdM(u^2 - i)})} \right) du \\ &= \int_0^{\infty} \frac{e^{iky u \sqrt{u^2 - 2i} + (3-2a)kx(u^2 - i)}}{\sqrt{u^2 - 2i}} \sum_{j=1}^M \frac{1}{e^{(2a-3)i\alpha j d} e^{kdj(u^2 - i)}} du \\ &\quad + \int_0^{\infty} \frac{e^{iky u \sqrt{u^2 - 2i} + (3-2a)kx(u^2 - i)}}{\sqrt{u^2 - 2i}} \frac{1}{(e^{(2a-3)i\alpha(M+1)d} e^{k(M+1)d(u^2 - i)} - e^{(2a-3)i\alpha M d} e^{kdM(u^2 - i)})} du \\ &= \sum_{j=1}^M \int_0^{\infty} \left[\sum_{n=0}^{\infty} a_n u^n \right] \frac{e^{(3-2a)i\alpha j d} e^{ky u(1+i)}}{e^{k(jd + (2a-3)x)(u^2 - i)}} du \\ &\quad + \int_0^{\infty} \frac{e^{iky u \sqrt{u^2 - 2i} + (3-2a)kx(u^2 - i)}}{\sqrt{u^2 - 2i} (e^{(2a-3)i\alpha(M+1)d} e^{k(M+1)d(u^2 - i)} - e^{(2a-3)i\alpha M d} e^{kdM(u^2 - i)})} du \\ &= \sum_{j=1}^M \left(\sum_{n=0}^{\infty} a_n I_{nj}^a \right) \\ &\quad + \int_0^{\infty} \frac{e^{iky u \sqrt{u^2 - 2i} + (3-2a)kx(u^2 - i)}}{\sqrt{u^2 - 2i} (e^{(2a-3)i\alpha(M+1)d} e^{k(M+1)d(u^2 - i)} - e^{(2a-3)i\alpha M d} e^{kdM(u^2 - i)})} du, \end{aligned}$$

where

$$I_{nj}^a = \int_0^{\infty} u^n \frac{e^{(3-2a)i\alpha j d} e^{ky u(1+i)}}{e^{k(jd + (2a-3)x)(u^2 - i)}} du.$$

Again rather than calculating the integrals I_{nj}^a directly, the formulas [31, Eqs. (4.146.1) and (4.146.2)] can be used in (32) to derive

$$I_{nj}^a = - \int_0^\infty (-u)^n \frac{e^{(3-2a)i\alpha jd} e^{-kyu(1+i)}}{e^{k(jd+(2a-3)x)(u^2-i)}} + A_j^a v_{n,j}^a,$$

where the weights $v_{n,j}^a$ are calculated as in (33) with

$$w_j^a = \frac{2(jd + (2a - 3)x)}{y(1 + i)} \text{ and } A_j^a = \sqrt{\frac{\pi}{k(jd + (2a - 3)x)}} e^{i\frac{ky^2}{2(jd+(2a-3)x)}} e^{ik(jd+(2a-3)x)} e^{(3-2a)i\alpha jd}.$$

Using the symmetry of the function $h(u)$ (cf. (35)), and proceeding as in (36) and (37), the sum $I_+^a + I_-^a$ can be rewritten as

$$\begin{aligned} I_+^a + I_-^a &= \sum_{j=1}^M A_j^a \sum_{n=0}^\infty \frac{h^{(n)}(0)}{n!} v_{n,j}^a \\ &+ \int_0^\infty \frac{e^{ikyu\sqrt{u^2-2i}+(3-2a)kx(u^2-i)} + e^{-ikyu\sqrt{u^2-2i}+(3-2a)kx(u^2-i)}}{\sqrt{u^2-2i}(e^{(2a-3)i\alpha(M+1)d} e^{k(M+1)d(u^2-i)} - e^{(2a-3)i\alpha M d} e^{kdM(u^2-i)})} du. \end{aligned}$$

The analogue of equation (57) is now

$$k_{mp} = \text{mod} \left(\frac{k}{p}, 1 \right), \text{ and } \alpha_{mp} = \text{mod} \left(\frac{\alpha}{p}, 1 \right),$$

(to be evaluated in multi-precision) and A_j^a can be rewritten

$$A_j^a = \sqrt{\frac{\pi}{k(jd + (2a - 3)x)}} e^{i\frac{ky^2}{2(jd+(2a-3)x)}} e^{(2a-3)ikx} e^{i2\pi j(k_{mp} + (3-2a)\alpha_{mp})}.$$

Finally, as in (39), $G_{\text{qp}}(x, y)$ can be expressed in the form

$$\begin{aligned} G_{\text{qp}}(x, y) &= -\frac{i}{4} H_0^{(1)}(kr) - \frac{1}{2\pi} \left(\sum_{j=1}^M A_j^1 \sum_{n=0}^\infty \frac{h^{(n)}(0)}{n!} v_{n,j}^1 + \sum_{j=1}^M A_j^2 \sum_{n=0}^\infty \frac{h^{(n)}(0)}{n!} v_{n,j}^2 \right. \\ &+ \int_0^\infty \frac{e^{ikyu\sqrt{u^2-2i}+kx(u^2-i)} + e^{-ikyu\sqrt{u^2-2i}+kx(u^2-i)}}{\sqrt{u^2-2i}(e^{-i\alpha(M+1)d} e^{k(M+1)d(u^2-i)} - e^{-i\alpha M d} e^{kdM(u^2-i)})} du \\ &\left. + \int_0^\infty \frac{e^{ikyu\sqrt{u^2-2i}-kx(u^2-i)} + e^{-ikyu\sqrt{u^2-2i}-kx(u^2-i)}}{\sqrt{u^2-2i}(e^{i\alpha(M+1)d} e^{k(M+1)d(u^2-i)} - e^{i\alpha M d} e^{kdM(u^2-i)})} du \right). \end{aligned}$$

References

- [1] Tsang L., Kong J. A. and Shin R. T., Theory of Microwave Remote Sensing (1985), (New York: Wiley).

- [2] Brekhovskikh L. M. and Lysanov Y. P., *Fundamentals of Ocean Acoustics* (Berlin: Springer-Verlag) (1982).
- [3] Rappaport T. S., *Wireless Communications: Principles and Practice*, 2nd ed. (2002), Englewood Cliffs, NJ: Prentice Hall.
- [4] Fortuny J. and Sieber A. J., Three-dimensional synthetic aperture radar imaging of a fir tree: First results, *IEEE Trans. Geosci. Remote Sensing.*, (1999) vol. 37, (1006-1014), Mar.
- [5] Herzig H. P., *Micro-Optics Elements, System, and Applications*. New York: (1998) (Taylor and Francis).
- [6] Reitich F. and Tamma K. K., State-of-the-art, trends, and directions in computational electromagnetics CMES, (2004), 5 287-294.
- [7] Sei A., Bruno O. and Caponi M., Study of polarization dependent scattering anomalies with application to oceanic scattering, *Radio Science*, 34, 2, (1999), 385-411.
- [8] Castillo P., Koning J., Rieben R., White D., A Discrete Differential Forms Framework for Computational Electromagnetics, *Computer Modeling in Engineering and Sciences*, (2004), volume 5, no. 4, (331-346), UCRL-JC-149836.
- [9] Fan M., Wang L., Steinhoff J., A new Eulerian method for the computation of propagating short acoustic and electromagnetic pulses, *Journal of Computational Physics*, (2000) Volume 157 , Issue 2, (683-706).
- [10] Chandler-Wilde S. N. and Zhang B., Electromagnetic scattering by an inhomogeneous conducting or dielectric layer on a perfectly conducting plate *Proc. Royal Soc. London Ser. A*, (1998), (454-519), 42.
- [11] Bleszynski, E., Bleszynski, M., Jaroszewicz, T., AIM: Adaptive integral method for solving large-scale electromagnetic scattering and radiation problems, *Radio Science*, (September-October 1996) Vol. 31, No.5, 1225-1251.
- [12] Chew W., Song J., Cui T., Velamparambil S., Hastriter S., and Hu B., Review of large scale computing in Electromagnetics with fast integral equation solvers, *Computer Modeling in Engineering and Sciences*, (2004) vol. 5, no. 4, pp. 361-372.
- [13] Twersky V., On the scattering of waves by an infinite grating, *IRE Trans. on Antennas Propagation* 4, (1956), 330-345.
- [14] Linton C. M., The Green's Function for the two-dimensional Helmholtz Equation in Periodic Domain, *Journal of Engineering Mathematics* 33, (1998), 377-402.
- [15] Petit R., *Electromagnetic Theory of Gratings*, Topics in Current Physics Vol. 22 of Berlin: Springer-Verlag, (1980).
- [16] Wait J. R., Reflection from a wire grid parallel to a conducting plane. *Can J. Phys.* 32 (1954), 571-579.

- [17] Van den berg P. M., Diffraction theory of reflecting grating, Appl. Sci. Res. 24, (1971) 261-293.
- [18] Lampe R., Klock P., Mayes P., Integral transforms useful for the accelerated summation of periodic, free-space Green's functions, IEEE Trans. Microwave Theory Tech 33 (1985) 734-736.
- [19] Mathis A. W., Peterson A. F., A comparison of acceleration procedures for the two-dimensional periodic Green's function, IEEE Trans. Antennas Propagat., 44, (1996), 567-571.
- [20] Linton C. M., Evans D., The interaction of waves with a row of circular cylinders. J. Fluid Mechanics 251 (1993) 687-708.
- [21] Petit R., From functional Analysis to fictitious sources in E.M. diffraction. In: MMET'94 Kharkov, (1994).
- [22] Jorgenson R. E., Mittra R., Efficient calculation free-space Green's function, IEEE Trans. Antennas Propagat., 38, (1990), 633-642.
- [23] Singh S., Richards W., Zinecker R., Wilton D., Accelerating the convergence of the series representing the free space Green's function, IEEE Trans. Antennas Propagat., 38, (1990), 1958-1962.
- [24] Nicorovici N.A., McPhedran RC, Petit R., Efficient calculation of the Green's Function for Electromagnetic Scattering by Gratings, Physical Review E, 49, 4563-4577, 1993.
- [25] Jordan K., Richter G., ShengP., An efficient numerical evaluation of the Green's function for the Helmholtz operator on periodic structures, J. Comp. Phys, vol 63, (1986), 222-235.
- [26] Twersky V., Elementary function representation of Schlomilch Series. Arch. Rational Mech. Anal., 8 (1961), 323-332.
- [27] McPhedran R. C., Nicorovici N. A., Botten L. C., Schlomilch series and grating sums, Journal of Physics A 38, 8553-8366, 2005.
- [28] Petit R., A tutorial introduction Electromagnetic Theory of Gratings (New York: Springer-Verlag) (1980) 140.
- [29] Abramowitz M. and Stegun I. A., eds. (1972), Handbook of Mathematical Functions with Formulas, Graphs, and Mathematical Tables, New York: Dover Publications (1964).
- [30] Capolino F., Wilton D. and Johnson W. A., Efficient Computation of the 2-D Greens Function for 1-D Periodic Structures Using the Ewald Method. IEEE Trans. Antenas Propagat. 53 (2005) 2977-2984.
- [31] Gradshteyn I. S., Ryzhik I. M., Tables of Integrals, Series, and Products, Academic Press, New York, (1980), 522p.
- [32] Faà di Bruno, C. F., Sullo sviluppo delle funzione., Ann. di Scienze Matem. et Fische di Tortoloni, 6, (1855): 479-480.

[33] Zhang S., Jin J., *Computation of Special Functions*, Wiley, (1996).